1 Introduction

Arctic sea ice has undergone immense inter-annual variability as well as longer term declines in recent decades. The Arctic is efficiently connected to the global climate system by the atmospheric/oceanic circulation in a mutual cause and effect relationship; (1) radiative and surface energy fluxes associated with Arctic sea ice loss directly impact the global energy budget (*Deser et al.*, 2015) and modify the large scale circulation of the atmosphere and ocean (*Varvus et al.*, 2017; *Overland et al.*, 2015; *Hwang et al.*, 2011; *Francis and Vavrus*, 2012) and (2) warming in distant regions of the climate system (i.e the tropics) are communicated to the Arctic via the movement of energy and moisture in the atmosphere (*Bekrayev et al.*, 2010; *Ding et al.*, 2014, 2017; *Woods and Caballero*, 2016). It is unclear whether the year-to-year variability and long term trends in Arctic sea ice decline are primarily controlled by local radiative and dynamic processes in the Arctic or result from remotely forced changes in the circulation (*Alexeev et al.*, 2005). Model predictions of future ice decline (*Blanchard-Wrigglesworth et al.*, 2011) and the polar amplification (*Kay et al.*, 2012) of surface temperature changes depend critically on adequately representing the processes responsible for sea ice decline in nature. Critical to this task is understanding and separating the processes that are forcing sea ice decline from those that are responding to sea ice loss in the observed record. This is the central task of the proposed work.

Specifically, the proposed work addresses two primary questions:

- How does sea ice loss impact the top of atmosphere (TOA) radiative budget of the Arctic? Are the radiative anomalies associated with ice loss caused by or are they forcing the sea ice anomalies?
- Does the energy transported into the Arctic by the atmospheric circulation force or respond to Arctic sea ice loss? Does the atmosphere import energy to initiate ice loss or does the heating of the Arctic atmosphere after an ice loss lead to atmospheric energy export?

While these two tasks involve different pieces of analysis – radiative versus dynamic – we emphasize that the two tasks are connected via the energy budget of the Arctic climate system; the atmospheric energy transport into the Arctic is balanced (excluding atmospheric energy storage) by the net heating of the Arctic by radiation and surface fluxes. Thus, the combined analysis of radiative and dynamic energy fluxes accompanying ice loss events provides insight into separating the processes that drive sea ice loss from the response to ice loss. The primary investigator has developed two novel techniques for (1) decomposing satellite derived radiative fluxes into contributions from surface versus atmospheric changes and (2) a new method for calculating the vertical structure of atmospheric energy fluxes into the Arctic that will provide insight into how the atmospheric circulation couples to the surface.

Preliminary analysis suggests two novel findings from the observed inter-annual variability of Arctic sea ice: (1) the direct (solar) radiative impact of sea-ice loss on the energy input to the Arctic is small (2 standard deviations, σ, = 1.5 W m^{-2}) compared to that of concomitant cloud changes (2σ = 2.3 W m^{-2} – Fig. 1) suggesting that previous satellite based analysis (*Pistone et al.*, 2014) likely overestimated the surface albedo feedback by more than a factor of 2 and (2) the net TOA radiative anomalies in the Arctic are much smaller (2σ = 4.3 W m^{-2}) than the input of energy to the Arctic via the atmospheric energy transport (2σ = 15.8 W m^{-2}) and surface fluxes (2σ = 14.5 W m^{-2}) suggesting that ice loss events are initiated by atmospheric and/or oceanic processes while the direct amplification via radiation provides only a modest feedback. We elaborate on how these two novel methods will allow a separation between the drivers and response to Arctic climate variability. This

proposal is organized into separate sections outlining the key science questions and methodology for each the radiative and atmospheric dynamics analysis but we emphasize here that the two sets of analysis will compliment each other to address the broader question of what processes drive sea ice changes in the coupled cryosphere/oceanic/atmospheric/radiative system and how adequately representing these physics in climate models informs longer term climate changes in the Arctic.

2 Radiative impact of Arctic sea ice loss: an observational estimate of the ice albedo feedback

Sea ice decline exposes the darker ocean surface and, thus, causes more solar radiation to be absorbed in the climate system. This effect is commonly termed the ice albedo feedback – a positive feedback whereby initial melting causes additional radiative input to the system which amplifies the initial ice loss. The magnitude of the ice albedo feedback differs substantially across global climate models (GCMs) due both to uncertainties in how much sea ice will retreat with warming and due to the radiative impact of the sea ice loss (*Qu and Hall*, 2005). Recent observations have improved our understanding of the Arctic surface energy budget (*Uttal et al.*, 2002) but there is very little observational work on the impact of sea ice anomalies on the top of atmosphere (TOA) radiative budget. Although surface energy budget changes are closely connected with sea ice loss, it can be argued that TOA changes are more relevant for understanding future climate change in the Arctic (and the global impact of those changes). The reason being, energy flux anomalies at the surface are often indicative of compensating changes in radiative heating of the surface versus the atmosphere that have little or no impact on the Arctic energy budget because of the rapid vertical adjustments of the coupled atmosphere/ocean/cryosphere system. For example, removing a reflective cloud over sea-ice will dramatically change the surface energy fluxes but has little effect on the climate system since solar radiation is reflected by the system in both cases. The TOA energy budget is closed with respect to radiative processes and tells the more revealing story about drivers and consequences of Arctic sea ice loss in the coupled climate system; is Arctic sea ice loss sustained by local radiative feedbacks or do changes in sea ice require changes in the input of energy into the Arctic via the atmospheric and oceanic circulation?

In order for changes in surface brightness to impact the TOA radiative budget, solar radiation must be transmitted downward through the atmosphere, reflected by the surface and then transmitted from the surface back to the TOA. Thus, the impact of melting ice on the Arctic energy budget depends not only on the changes in surface brightness but also on the climatological optical properties of the atmosphere (i.e. on solar reflectors such as clouds and aerosols and solar absorbers such as water vapor). Recent work (*Donohoe and Battisti*, 2011) has demonstrated that, in the global average, the impact of surface albedo on TOA albedo is reduced by a factor of three due to the solar opacity of the atmosphere. That work focused on the global climatology, but also suggested that the impact of Arctic surface albedo changes on the TOA radiation would be damped by a factor of five in the absence of concurrent cloud changes. The reason being, clouds are ubiquitous in the Arctic and, as a result, changes in surface brightness seen from the view of the TOA (i.e. the TOA energy budget) are masked by the cloud cover.

While the Arctic ice albedo feedback has been thoroughly studied in climate models using ensembles of forced simulations (*Bony et al.*, 2006) and radiative kernel techniques (*Soden and Held*, 2006) there have been very few observationally based studies on the ice albedo feedback (*Wang and Key*, 2005; *Kato et al.*, 2006). *Pistone et al.* (2014) used the interannual covariance between

surface albedo anomalies and TOA radiation to deduce that sea ice decline in recent decades has resulted in more the 6 W m^{-2} additional solar radiation absorbed in the Arctic climate system. While novel in its use of the observations, this study assumed that the TOA radiation that co-varies with the surface albedo were caused by changes in the surface albedo – a logical connection but one that potentially confuses cause and effect. An alternative explanation is that radiative anomalies are either directly forcing sea ice loss or are responding to processes connected with the sea ice loss. For example, increases in downward solar radiation at the surface due to decreased cloud cover could initiate sea ice loss (*Kay et al.*, 2008; *Choi et al.*, 2014). Alternatively, sea ice loss may lead to decreased cloud cover by way of reduced stability in the boundary layer (*Schweiger et al.*, 2008). A third alternative is that sea ice variability is triggered remotely by anomalous atmospheric energy and moisture transport into the Arctic (*Ding et al.*, 2017; *Woods and Caballero*, 2016) resulting in a warming and moistening of the atmosphere. The latter would affect the temperature, humidity and static stability of the atmospheric column and, thus, the cloud cover (fraction, height, optical thickness) and radiation (both SW and longwave) at the TOA. In all three cases above, calculating the ice-albedo feedback from statistical regressions between TOA radiation and sea ice extent results in a portion of the TOA radiative anomalies that result from the processes other than the sea ice variability to be mistakenly be identified as resulting directly from the sea ice variability itself. The aim of the proposed work is to achieve a better understanding of the connection between observed TOA radiative anomalies and sea ice loss by separating the radiative anomalies that directly result from ice loss from the radiative components that co-vary with Arctic ice loss events.

The *Pistone et al.* (2014) estimate of Arctic radiative changes associated with sea ice loss translates to a global mean positive radiative feedback of 25% of the forcing, suggesting a substantial (25%) amplification of future global temperature change by the Arctic ice albedo feedback which may be erroneous. Furthermore, the amplitude of the Arctic surface albedo feedback is the primary driver of model differences in the polar amplification of surface temperature changes (*Kay et al.*, 2012). Current observational estimates put the Arctic ice albedo feedback at the upper end of the model range and, thus suggest that future climate change will be strongly polar amplified. These observational estimates may be biased high if cloud processes indeed play a significant role in sea ice loss. Thus, future estimates of polar amplification, sea ice loss and the impact of ice loss on mid-latitude atmospheric circulation rely on understanding the radiative anomalies that result directly from sea ice loss versus those that are forcing or co-varying with sea ice extent. Furthermore, if the satellite record is used calibrate the Arctic ice-albedo feedback in climate models, the models will be overly sensitive if the radiative impact of cloud changes concomitant to the ice loss is not removed from the satellite based estimate of the ice albedo feedback.

2.1 Methodology

The portion of incident solar radiation (insolation) that is not reflected back to space is absorbed within the climate system – either at the Earth's surface or within the atmospheric column. Therefore, the ratio of upwelling shortwave (SW) radiation at the TOA to insolation – the planetary albedo (α_P)– determines how much SW radiation is absorbed in the climate system. Over the Arctic, reflection off of clouds and reflection off the bright surfaces both contribute to α_P and the relative contributions of each are difficult to disentangle from radiation measurements at the TOA only (i.e. from satellites). However, simultaneous radiative measurements at the surface and TOA provide additional constraints on partitioning α_P since reflective clouds will simultaneously in-

crease upwelling SW at TOA and reduce downwelling SW at the surface whereas a bright surface will only (neglecting higher order effects) impact the former. Here, we propose to use simultaneous observational estimates of radiative fluxes at the TOA and surface to partition the satellite derived planetary albedo into surface and atmospheric contributions in order to derive a more comprehensive observationally based estimate of the Arctic surface albedo feedback.

Donohoe and Battisti (2011) recently developed a method for partitioning the observed climatological α_P into atmospheric and surface contributions using the CERES satellite data alongside the accompanying surface radiative flux products (*Kratz et al.*, 2010). In short, their method relies on a single layer atmosphere, isotropic SW radiation model which assumes that, independent of whether light is traveling upward or downward, a fixed fraction of the radiation incident on the atmosphere is absorbed and reflected by the atmospheric layer. For example, as light passes downward through the atmosphere, a fraction R is reflected back to space and a fraction A is absorbed within the column with the remainder (1-R-A) transmitted to the surface where it can be reflected by the surface albedo (α). The same processes is repeated for the upwelling radiation reflected by the surface and the reflections are continued indefinitely. The result is a set of predictive equations for the upward and downward SW fluxes at the TOA and surface given values of the fractional reflection (R) and absorption (A) of the single atmospheric layer. Given satellite based measurements of the radiative fluxes at the TOA and surface, one can solve the system of equations analytically and uniquely for A and R. One can then identify the contribution of atmospheric reflection ($\alpha_{P,ATMOS}$) versus surface reflection ($\alpha_{P,SURF}$) to the reflected SW radiation at the TOA. In order for the surface to contribute to α_P, the insolation must be transmitted through the atmosphere to the surface, reflect off the surface and then be transmitted back through the atmosphere to the TOA. Therefore, $\alpha_{P,SURF}$ is equal to α times the atmospheric SW transmissivity squared which is 0.34 in the global average and 0.2 over the Arctic. This method is simple to implement, physically based, compares well with comprehensive radiative transfer calculations (Section 4.1.2) and can be applied to observational data products and model output alike to allow for a comparison between observed and modeled processes. In the proposed work, we will apply this same methodology to the interannual and interseasonal variability of the Arctic planetary albedo over the CERES era (2000-2017). The end goal is to link sea ice variability with the surface contribution to planetary albedo to directly assess the ice albedo feedback.

2.2 Preliminary results: sea ice loss has a small direct impact on TOA radiation

We begin our analysis by comparing the magnitude of anomalies in absorbed shortwave radiation (ASR = net SW at the TOA) in the Arctic with that expected if the surface albedo anomalies were realized at the TOA (i.e. if the atmosphere were transparent to SW radiation resulting in an ASR anomaly equal to the surface albedo times insolation). During years with low Arctic sea ice (e.g. 2008, 2012) the lowered surface albedo would result in an ASR anomaly of order 4 W m^{-2} averaged over the Arctic (poleward of 60°N) domain (blue line of Fig. 1A). The realized ASR anomalies during ice loss events (red line) are more modest than those expected from surface changes in the limit of a SW transparent atmosphere; on average a 1 unit change in Arctic average surface albedo is accompanied by a 0.47 unit change in α_P. *Pistone et al.* (2014) interpreted this number to represent the actual impact of α changes on ASR. However, the isotropic SW model suggest that the α_P change that is directly due to change in surface albedo ($\alpha_{P,SURF}$) is significantly smaller in magnitude than the total change in α_P (the pink line in Fig. 1B); the regression slope between

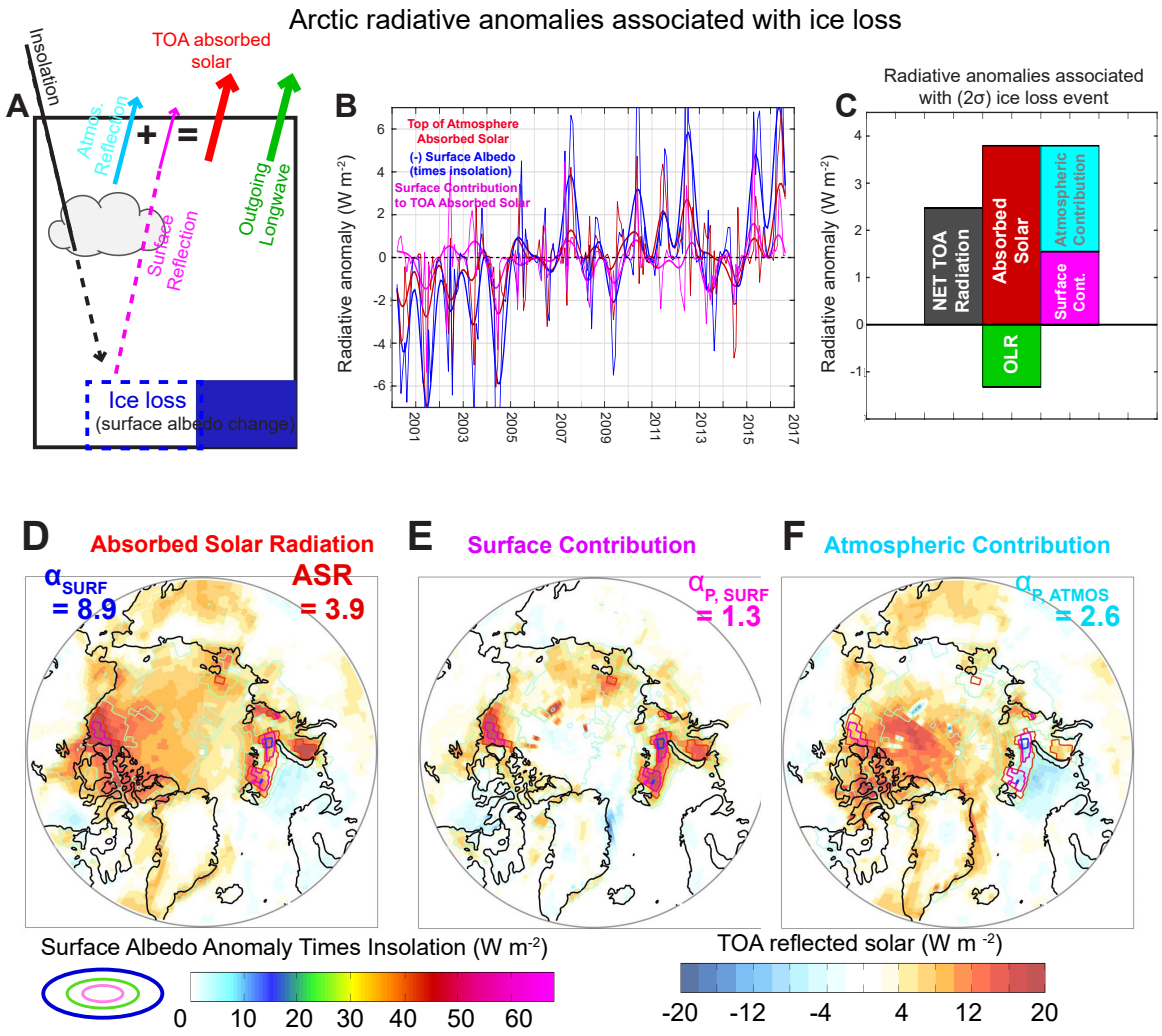

Figure 1: (A) Schematic for decomposing solar fluxes at the top of atmosphere into contributions from surface albedo (purple line) and atmospheric reflection (cyan line). (B) Time series of anomaly in Arctic averaged (blue) surface albedo, (red) TOA absorbed solar radiation (purple) surface contribution to TOA absorbed solar radiation from CERES. All data are expressed as Arctic averaged radiative anomalies into the TOA by multiplying the (negative of) surface/planetary albedo anomalies by insolation. Thin lines are monthly means and thick lines are low pass filtered with a 1 year cutoff period. (C) Arctic averaged radiative anomalies associated with "typical" (2σ) ice loss event. The (gray) net radiation at TOA is subdivided into (green) longwave and (red) shortwave contributions and the shortwave is further decomposed into (purple) surface and (cyan) atmospheric contributions to ASR. (D-F) Spatial maps of (D) absorbed solar radiation – ASR, (E) surface contribution to ASR (F) atmospheric contribution to ASR associated with an Arctic wide α anomaly. The contours show the spatial map of the surface albedo map with contour interval of 15 W m^{-2} and the domain average values (in W m^{-2}) are given in the upper corners.

$\alpha_{P,SURF}$ and α is 0.2. This result suggests that looking at statistical correlations between α and α_P over the Arctic would overestimate the surface albedo feedback by a factor of 2.5. *Cao et al.* (2015) pointed out a similar disconnect between satellite based estimates of the surface albedo feedback and those calculated from radiative kernels but concluded that the radiative kernels underestimated the feedback in nature due to cloud masking. We note that, based on CERES climatology, less than 45% of the insolation makes it to the surface in the Arctic*. Therefore, in order for a one unit change in α to directly cause a 0.47 unit change in the α_P of the Arctic (as deduced from statistical correlations) more than all of the radiation reflected off the surface must be transmitted to space – a result that is not physically plausible.

We now analyze and compare the spatial pattern of ASR and surface albedo anomalies associated with an Arctic wide sea ice retreat by defining the map of anomalies in a "typical" Arctic wide low α (ice retreat) event. A "typical" pattern is defined by regressing a normalized index of the Arctic averaged α on the α anomaly at each grid point (we multiply by -2 to represent a 2σ retreat event). It can be thought of as the average anomaly that occurs at each gridpoint when a 2σ basin wide reduction in α occurs – similar results are found from compositing around low versus high α events. We show the α anomalies in units of the changes in ASR expected in the limit of a SW transparent atmosphere accomplished by multiplying by (-) insolation as shown by the contours in Fig. 1D-F). The spatial pattern of α in a "typical" ice retreat event features local maxima around the sea ice edge concurrent with the region of ice loss with amplitudes of 60 W m^{-2} with minimal signal over the central Arctic where there is little sea ice loss. In contrast, the associated ASR anomalies (colors in Fig. 1D) are more spatially diffuse with nearly equal magnitude anomalies over the climatological sea ice edge and central Arctic. Moving from the ice edge North of the Canadian Arctic to the central Arctic, the α anomalies decrease by a factor of 5 but the ASR anomalies are nearly spatially invariant (c.f. the contours and colors in Fig. 1D). Overall, there is a spatial mismatch in the pattern of α and ASR anomalies. This suggests that there are changes in atmospheric reflection and/or absorption of SW radiation that are concurrent with the sea ice anomalies.

Indeed, the isotropic SW model ascribes the changes in ASR around the sea ice edge to $\alpha_{P,SURF}$ changes and the more spatially diffuse ASR anomalies over the central Arctic to $\alpha_{P,ATMOS}$ changes (c.f. the colors in Figs. 1 E and F). As expected, the spatial pattern of ASR due to $\alpha_{P,SURF}$ anomalies mimics that of α anomalies with reduced magnitudes (by a factor of 3-5) suggesting that the changes in $\alpha_{P,SURF}$ are being dictated by the surface brightness changes attenuated by the climatological atmospheric SW opacity. A "typical" Arctic wide α anomaly (2σ) is associated with an additional 3.8 W m^{-2} SW radiation absorbed in the Arctic, 1.5 W m^{-2} of which is due to $\alpha_{P,SURF}$ changes and 2.3 W m^{-2} of which is due to changes in $\alpha_{P,ATMOS}$ (Fig. 1C). This analysis again suggests that if one were to merely look at regressions between the α and ASR over the observational record (*Pistone et al.*, 2014)), the direct impact of sea ice anomalies on ASR would be overestimated by a factor of 2-3. We further note that the α_P anomaly over the central Arctic is larger in magnitude than the α anomaly in that region (c.f. the magnitude of the colors and contours in Fig. 1D). Even in the limit of a completely transparent atmosphere, the α anomalies can not cause such a large α_P anomaly. All evidence suggest that the ASR anomaly associated with sea ice loss is only partly a direct result of the changes in surface brightness and that other important

*The ratio of downwelling SW radiation at the surface to insolation is 0.45 in the CERES data set. This includes contributions from multiple reflections off of the surface and clouds and, thus, 0.45 is an upper bound on the downwelling SW transmissivity of the Arctic

processes involving atmospheric constituents (i.e. clouds and water vapor) must be involved. We will identify these processes and thereby achieve a better understanding of the processes that drive sea ice loss in the proposed work.

3 Atmospheric energy fluxes associated with sea ice retreat

In the annual mean climatology, TOA radiation cools the Arctic by approximately 100 W m^{-2}. This energy loss is nearly (90 W m^{-2}) balanced by energy input into the Arctic by the large scale atmospheric circulation (*Serreze et al.*, 2007) – commonly referred to as F_{WALL}. The ocean energy transport into the Arctic is an order of magnitude smaller (10 W m^{-2}). We wish to understand the year-to-year variability of the Arctic energy budget. Specifically, what energetic processes initiate ice loss events and how does the ice loss itself alter the Arctic climate system's energetics? Recently, *Donohoe and Battisti* (2013) developed a novel methodology for calculating the vertical structure of atmospheric energy fluxes from the observational reanalyses. This methodology which is detailed in Section 4.3 will allow a calculation of the year-to-year variability of Arctic atmospheric heating that results from anomalous atmospheric heat flux divergence as well as an understanding of how that heating is coupled to the surface energy budget and sea ice variability.

The magnitude of F_{WALL} variability can be compared to that of Arctic radiation and surface energy fluxes to glean understanding of the processes that drive Arctic climate variability. We demonstrate below that radiative variability in the Arctic is substantially smaller than either F_{WALL} or surface energy fluxes and we argue here that this result implies that radiative processes can not be the primary driver of Arctic sea ice loss as follows. For the sake of argument, assume that all of the radiative variability results from changes in surface brightness due to changes in ice extent – a result our previous analysis suggest is an overestimate/upper bound of the impact of ice loss on radiation. This enhanced absorbed solar radiation is balanced by three atmospheric energy loss processes: (1) a downward surface energy flux, (2) energy storage in the atmosphere associated with atmospheric warming (and moistening) and, (3) anomalous energy export to lower latitudes (i.e. reduced F_{WALL}). Therefore, if radiative processes were the primary driver of Arctic climate variability, one would expect the variability in TOA radiation to exceed that in F_{WALL} and surface heat fluxes. Thus, our results suggest that radiative processes are not the primary driver of Arctic variability.

To frame our discussion of how energetic analysis will reveal the primary mechanism that drives Arctic ice loss, we formulate two limiting (i.e. overly simplified) models of how Arctic ice loss events might be initiated: (1) ice loss is triggered by processes internal to the Arctic such as changes in ocean stratification associated with surface wind stress anomalies (*Zhang et al.*, 2013) or changes in the lateral (*Steele et al.*, 2010) ocean heat transport (Fig. 2B) or (2) ice loss is initiated by processes remote to the Arctic such as anomalous atmospheric energy (*Ding et al.*, 2017) and/or moisture (*Woods and Caballero*, 2016) transport into the Arctic (Fig. 2C). We argue that these two limiting models have distinct energetic signatures in the magnitude and phasing of Arctic wide energy fluxes relative to the timing of sea ice loss. Thus, analysis of the phase and amplitude of the Arctic energy budget during ice loss events can distinguish between the cause and impact of ice loss events. If ice loss is initiated by internal processes (Fig. 2B), the resultant ice loss will lead to anomalous upward (turbulent) energy fluxes to the atmosphere and atmospheric warming. Subsequently energy is lost radiatively to space and anomalous energy is fluxed equatorward in the atmosphere (F_{WALL} is reduced) following the ice loss event. In contrast, if ice loss is initiated

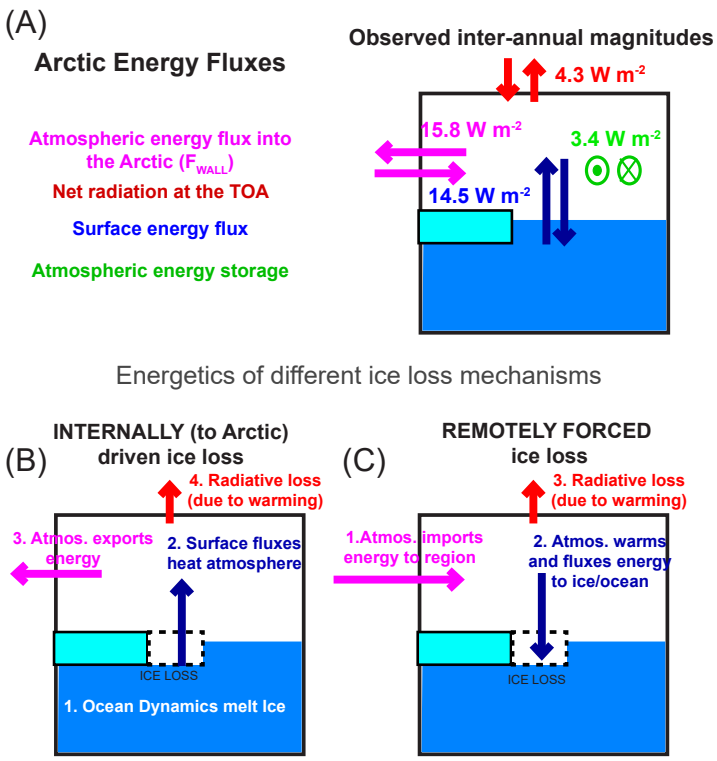

Figure 2: (A) Schematic representing the year-to-year magnitude (2σ) calculated from the observations: (purple) atmospheric energy flux across 60° and (green) atmospheric column energy tendency both calculated from NCEP reanalysis, (red) TOA net radiation from CERES and, (blue) net surface energy calculated as the residual of the other terms. (Bottom panels) Schematic of the direction of anomalous energy fluxes concomitant with ice loss driven by (B) oceanic/surface processes and (C) atmospheric circulation.

by anomalous poleward atmospheric energy transport (enhanced F_{WALL}), the resultant atmospheric heating will lead to downward surface energy fluxes (*Burt et al.*, 2016) into the ocean as well as radiative energy loss following the ice loss event (Fi. 2C). Thus, both the sign and phasing of the surface energy fluxes and F_{WALL} during ice loss events distinguish between the two proposed mechanisms of ice loss. We emphasize that this theoretical construct of ice loss events is overly simplified and that ice loss events likely result from a combination of specific coupled atmospheric/oceanic/cryospheric/radiative processes and, indeed, preliminary analysis suggests that different Arctic ice loss events may have different energetic signatures. However, the large scale energy budget of the Arctic associated with ice loss events facilitates a comparison of the relative importance of local Arctic processes (e.g. ocean dynam ics and ice-albedo feedbacks) versus remote forcing (e.g. F_{WALL}) through the common metric of energy fluxes.

3.1 Preliminary results and science questions

Preliminary calculations of F_{WALL} using the methodology of *Donohoe and Battisti* (2013) on the NCEP (*Kalnay et al.*, 1996) and ERA Interim (*Dee et al.*, 2011) find two novel results that provide new insights into separating the processes that drive sea ice variability from those that respond to ice loss:

- (1) The inter-annual variability of F_{WALL} (2σ) heats/cools the Arctic climate system by approximately 16 W m^{-2} (F_{WALL} divide surface area of Arctic–Fig. 2A) and exceeds both the TOA radiative variability (≈ 4 W m^{-2}) and changes in atmospheric energy content (≈ 3 W m^{-2}) substantially. As discussed in the previous subsection, this finding suggests that – even if all of the radiative anomalies were a direct result of the ice loss– radiative processes can not be the primary driver of Arctic sea ice variability. We reiterate that argument here: if the ra-

diation was the primary driver of Arctic climate variability, the anomalous radiative heating of the Arctic would be expected to warm the Arctic atmosphere leading to reduced F_{WALL} and an F_{WALL} that damps but *is smaller in magnitude* than the radiative anomaly. Rather, our findings suggest that the dominant Arctic energy balance at the interannual timescale is between atmospheric energy transport into Arctic balanced by energy exchange between the ocean and atmosphere. The cause and effect of that relationship and connection to sea ice loss is unclear and we hope to gain further insight in the proposed work.

- (2) The year-to-year variability of F_{WALL} includes a significant contribution ($\approx$40%) from the stratospheric circulation (right panels of Fig. 3) that *most likely has confused/obscured the connection between Arctic sea ice and the atmospheric circulation*. This stratospheric contribution was previously suggested by *Overland and Turet* (1994) and our methodology provides an unprecedented vertical structure of F_{WALL} over the satellite era. We speculate that stratospheric energy fluxes most likely make a small imprint on the surface climate in the absence of a downward propagation method (*Baldwin and Dunkerton*, 1998). Thus, *removing the stratospheric component from* F_{WALL} to isolate the tropospheric portion of F_{WALL} – that is efficiently coupled to the surface– may lead to new insights into the connection between sea ice and atmospheric circulation.

The broader goal of the proposed work is to understand the relative roles of atmospheric dynamics, ocean processes and radiative processes in initiating and amplifying Arctic sea ice anomalies in the observed record. Furthermore, how does the current generation of climate models capture the variability in atmospheric circulation and the radiative coupling between the TOA and the surface in the Arctic? How does their ability to do so affect predictions of future change and variability? Are sea ice anomalies a result of local radiative processes (feedbacks and forcing) or a consequence of changes in the energy input to the Arctic via the atmospheric energy transport and are the same mechanisms responsible for the interannual variability likely players in the response to global warming? More importantly, can we use observational constraints to guide which models accurately represent the dominant physics of the Arctic and are more likely to provide useful future prediction of long term Arctic climate change.

4 Proposed work

The preliminary results reported in the previous section suggest that the surface albedo feedback of Arctic sea ice loss is highly attenuated by the atmospheric SW opacity and that previous observational estimates of the surface albedo feedback (*Pistone et al.*, 2014) may have confused concurrent changes in atmospheric properties with the direct impact of surface albedo on TOA radiation. This is an important finding because it suggests that these concurrent changes in atmospheric properties may have played a role in driving or modifying the sea ice losses. We propose to further investigate this finding by exploring the atmospheric conditions that lead to reduced cloud reflection when sea ice retreats, the consistency of the these findings between the CERES data set and other observations and the sensitivity of the conclusions reached to the assumptions made in the isotropic SW model. Most importantly, we wish to understand if the α_P anomalies associated with Arctic sea ice retreat are a result of the sea ice retreat –by way of changing cloud cover or atmospheric moisture content – or are byproduct of processes that force the ice retreat. Ultimately, this question is embedded in the larger question of what physical processes are responsible for the interannual and forced Arctic sea ice retreat and the associated polar amplification of Arctic surface temperature

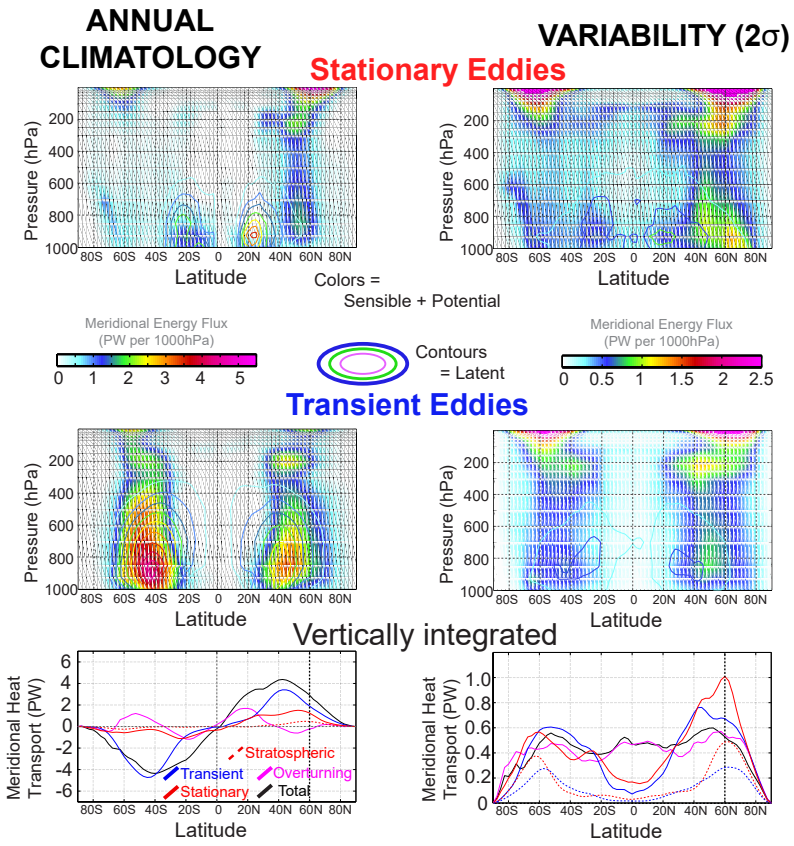

Figure 3: The vertical and latitudinal structure of (left columns) climatological and (right columns) interannual variations (2σ of monthly anomalies) of poleward atmospheric energy transport in the (top) stationary eddies and (middle) transient eddies. The dry (potential plus sensible) energy transport is shown in colors and the contours are the moisture (latent) transport with the same colorbar for each column. The units are PW per 1000 hPa such that vertically averaging the upper panels gives the resultant vertically and zonally integrated atmospheric energy flux in PW (10^{15} W) shown in the lower panel. The vertically integrated energy transport also includes a contribution from the (purple) mass overturning circulation (to which no vertical structure is ascribed) and subdivides the transient and stationary eddies into contributions from the stratospheric circulation – defined as above 200 hPa (dashed blue and red lines respectively).

change (*Holland and Bitz*, 2003).

Based on the preliminary results we therefore formulate the following working hypothesis;

There are concomitant changes in atmospheric reflection and/or absorption when sea ice retreats that are either a result of the ice retreat or are emblematic of the large scale forcing that initiates the ice loss.

But where does this variation in atmospheric radiative properties come from? Is it connected to variability in the large scale circulation of the atmosphere or a local adjustment to surface variations? We begin by describing the proposed analysis to diagnose the nature of the cloud and atmospheric optical properties accompanying the sea ice loss including the methodological uncertainties associated with our application of the isotropic shortwave model to the CERES data (Section 4.1). Next, we propose analysis of the connection between sea ice variability and the energy transport into the Arctic by atmospheric motions (Section 4.2). Lastly, we discuss how we will use an ensemble of climate model simulations to analyze the physical processes that initiate, sustain and damp Arctic sea ice variability and if the same physical processes are responsible for the long term trends in Arctic sea ice loss due to external forcing (Section 4.3).

4.1 The connection between sea ice loss, cloud anomalies, and atmospheric optical properties

The isotropic SW model suggested that atmospheric reflection and/or absorption co-varies with Arctic sea ice decline. Here we look for signatures of that co-variance in the cloud and water vapor fields and assess the observational uncertainties on the relationship between sea ice retreat and TOA

radiation.

4.1.1 Cloud changes accompanying sea ice anomalies

The multispectral Moderate Resolution Imaging Spectroradiometer (MODIS) is co-located with the CERES instrument on the AQUA and TERRA satellites and, thus, can be used to provide cloud observations alongside the CERES radiation data (*Platnick et al.*, 2003). We will analyze cloud fraction, cloud optical thickness, derived water path and cloud top pressure and the co-variance of these fields with sea ice and TOA radiation. The detection of cloud properties by MODIS over ice is known to be more problematic than over open ocean due to the similarity of thermal and SW optical properties of clouds and surface ice (*Liu et al.*, 2010). This is potentially problematic for our analysis since we aim to explicitly look at the co-variability of ice and clouds and this bias maybe confused for actual variability of the cloud fields. For this reason, we will also incorporate data from CloudSat radar and CALIPSO lidar in the synchronously flying A-train constellation of satellites (*Stephens*, 2008). Cloudsat Calipso data have limited spatial and temporal resolution and are only available since 2006 but provide an unprecedented vertical profile of cloud properties that is devoid of the contamination by changes in the surface brightness. *Kato et al.* (2011) recently developed a merged MODIS/CERES and CloudSat/Calipso product of cloud profiles based on a joint analysis of the different satellite products. We will compare the co-variability of sea-ice and clouds/atmospheric reflectance in this merged product over 2006-2014 period and compare with that in the MODIS product to determine if and how cloud detection in MODIS is biased by concurrent changes in surface brightness. Understanding and adjusting for this potential bias will allow us to analyze the co-variability of clouds and sea ice over the entire CERES era.

Additionally, we will analyze the relationship between sea ice, TOA radiation and cloud properties in the extended Advanced Very High Resolution Radiometer (AVHRR) Polar Pathfinder (APP-x) dataset (*Wang and Key*, 2005). This dataset is available from 1982 to present day and includes both TOA and surface radiative fluxes as well as cloud properties derived from the cloud and surface parameter retrieval (CASPR) system for polar AVHRR (*Key*, 2002). While the CERES data provides the most observationally constrained estimate of TOA radiation, we will analyze the APP-x data for consistency of our scientific findings and assess the potential for extending the observationally based calculation of the Arctic surface albedo feedback back to 1982 to provide a better context for the relative amplitudes of observed trends and natural variability of TOA radiation and sea ice.

4.1.2 Methodological uncertainties: accuracy of CERES surface albedo and isotropic SW model

As part of our investigation we will examine whether methodological problems may have contributed to the conclusion that TOA radiative anomalies associated with sea ice retreat are primarily due to changes in atmospheric as opposed to surface optical properties. Several possibilities exists: 1. The CERES product is underestimating the spatial extent of the surface albedo anomalies, especially over the central Arctic where melt ponds may exists, 2. The isotropic SW model is mis-attributing changes in α_P between changes in surface and atmospheric processes due to shortcomings of the isotropic and single layer assumptions. We believe neither of these shortcomings are effecting our preliminary conclusions based on comparison with the results of *Choi et al.* (2014)

and *Kay et al.* (2008) and the performance of the isotropic model against a comprehensive radiative transfer model (discussed below). Nonetheless, we briefly explore the methodological uncertainties here.

Accuracy of CERES surface albedo

The CERES surface albedo is derived by first identifying the cloud scene from MODIS and then "tuning" the surface albedo (via a Lagrange Multiplier minimization technique) alongside atmospheric optical properties so that the TOA fluxes in the radiative transfer model (*Fu and Liou*, 1993) best match those observed by the CERES instrument for each cloud scene (*Rutan et al.*, 2006). Potential problems with the CERES α retrievals include: 1. Faulty cloud scene identification 2. Changes in the spectral shape of the surface albedo – which is prescribed from look up tables based on the initial scene identification and thereafter multiplied by a scalar (representative of the broadband α) in the "tuning" process. Despite these limitations, the CERES derived surface radiative budget agree with ground based measurements to within 2% (*Rutan et al.*, 2001). The goal of the proposed work is to evaluate the CERES Arctic sea ica albedo and its variability against alternative measurements of Arctic α.

We will compare the spatial pattern of albedo anomalies associated with sea ice retreat in the CERES data with that from the MODIS MCD43 (*Schaaf et al.*, 2002) product which is derived from measurements on the same satellite as the CERES instruments but provides additional spectral and angular dependencies of the surface albedo (*Lucht*, 1998). Additionally, *Rosel et al.* (2012) recently developed a (spectral unmixing) technique for melt pond detection from MODIS that we will use to assess if the CERES data adequately captures the spatial extent of surface darkening during a sea ice retreat event. Lastly, we will pursue the hypothesis that improper cloud scene identification by MODIS is leading to an underestimation of CERES α anomalies by comparing the CERES α anomalies to those derived using additional inputs of cloud vertical profiles from CALIPSO by comparison to the merged CERES-CALIPSO-MODIS product (*Kato et al.*, 2011) over the common time period (2006-2014) which includes the widespread sea ice retreat events of 2007 and 2012. Although MODIS cloud detection biases have been examined before (*Liu et al.*, 2010), here we will specifically focus on biases in CERES surface radiation products.

Validation of the isotropic SW model using radiative transfer calculations

The partitioning of SW radiative fluxes at the TOA into surface and atmospheric processes relies on the assumptions of the single layer isotropic model: (1) The atmosphere can be represented by a single layer and (2) Atmospheric reflection and absorption are isotropic and can be represented by a single fraction representative of broadband optical properties. We emphasize that the preliminary conclusions found here – that a substantial portion of the TOA radiative anomalies associated with sea ice decline are not a direct consequence of the surface albedo feedback – are supported by findings that do not rely on the isotropic SW model including: (1) The spatial mismatch between the surface and TOA albedos in a "typical" ice retreat event and (2) The order 4-5 atmospheric attenuation of the impact of α anomalies to α_P expected from the mean state atmospheric opacity in the Arctic. Nonetheless, we will analyze the accuracy of the partitioning of α_P into atmospheric ($\alpha_{P,ATMOS}$) and surface ($\alpha_{P,SURF}$) contributions in the SW isotropic model by evaluation against an ensemble of experiments in a radiative transfer model. Specifically, we will input various atmospheric profiles representative of the Arctic (i.e. different cloud types, heights and cloud fractions) into the Streamer radiative transfer model (*Key and Schweiger*, 1998). For each atmospheric profile, we will vary the α from 0 to 1. We will then use the TOA and surface radiative fluxes from Streamer output to partition α_P into $\alpha_{P,ATMOS}$ and $\alpha_{P,SURF}$ via the isotropic model. If the isotropic

model is working properly, all changes in TOA radiation that result from the imposed sweep across α in Streamer should be attributed to $\alpha_{P,SURF}$, since the atmospheric optical properties are fixed. These experiments will allow us to evaluate the isotropic SW model against the behavior of a more comprehensive radiative transfer model and assess the uncertainties of decomposing the observed α_P into $\alpha_{P,ATMOS}$ and $\alpha_{P,SURF}$ over the Arctic.

A similar evaluation of the isotropic model was performed by *Donohoe and Battisti* (2011). They found that the model performed very well globally and that the isotropic and single layer assumptions were consistent with the radiative transfer calculations. The Arctic climate system presents a unique challenge in SW radiative transfer because both the clouds and surface are highly reflective. As a result, radiative fluxes at the TOA and surface include contributions that have reflected back and forth between the surface and clouds. These interactions are explicitly included in the isotropic SW model which allows for an infinite number of reflections between the surface and clouds (by way of an analytic solution). Preliminary results using the above methodology suggests that the isotropic model is particularly well suited for the Arctic atmosphere; changes in α_P that result from a sweep across αvalues with fixed atmospheric optical properties in Streamer are primarily ($> 95\%$) attributed to $\alpha_{P,SURF}$. These preliminary results suggest that the isotropic SW model is an excellent tool for improving observational evaluations of the Arctic surface albedo feedback and improving our understanding of the root cause of sea ice retreat. We emphasize that the overarching strategy of this proposal is to use the limited number of fields directly observed by satellites to isolate the radiative impact of Arctic sea ice loss. For this reason, we choose not the use a full radiative transfer code (Streamer) for our primary calculations because the number of input fields (i.e. clouds, humidity) to do so would result an end product that is more model-like than observationally constrained.

4.2 Atmospheric energy transport into the Arctic accompanying sea ice loss

We will use the method of *Donohoe and Battisti* (2013) to decomposes the atmospheric energy fluxes into components associated with the mass overturning circulation of the atmosphere, stationary eddies (associated northward flow at one longitude and compensating southward flow at another longitude) and transient eddies (storms) – based on the pioneering work of *Lorenz* (1953). The computation of F_{WALL} via this methodology is in very close agreement with the more standard mass flux corrected form of the calculation (*Trenberth and Stepaniak*, 2003) but allows for the added insight into the vertical structure of atmospheric energy flux anomalies and circulation structures that give rise the F_{WALL} anomalies.

In the proposed work, we will perform similar calculations of F_{WALL} using the NASA Modern-Era Retrospective Analysis version 2 (MERRA2– *Gelaro et al.*, 2017) to accompany the existing calculations with ERA-interim (*Dee et al.*, 2011) and NCEP (*Kalnay et al.*, 1996) reanalysis to check for the consistency of the calculations between reanalyses and the robustness of our scientific conclusions and interpretations. Preliminary results suggests that F_{WALL} calculated from NCEP and ERA Interim agree remarkably well in both the climatology and year-to-year variability (R=0.7) with the exception of the energy transport associated with the zonal mean mass overturning circulation. Furthermore, we will look for signatures of the circulation on the large scale cloud fields, radiation and the phase relationship with sea ice retreat in order to separate cause and effect and isolate the mechanism responsible for sea ice retreat from those processes that respond to the ice loss. Specifically, we will ask if isolating the lower tropospheric energy transport from the ver-

tically integrated F_{WALL} and/or isolating the moist energy fluxes leads to a clearer understanding of whether F_{WALL} is forcing or responding to Arctic sea ice anomalies.

4.3 GCM studies

While the proposed study is primarily observationally based, we will compare our observational findings on the impact of Arctic sea ice variability on TOA radiation and the physical processes responsible for sea ice decline with the same behavior in the suite of GCMs participating in the Coupled Model Intercomparison Project Phase 5 (*Taylor et al.*, 2012). We will analyze the internal variability of Arctic sea ice in pre-industrial (PI) simulations and the response of sea ice to anthropogenic forcing in strongly forced (instantaneous CO_2 quadrupling simulations– hereafter $4XCO_2$). Specifically, we will partition α_P in the models into $\alpha_{P,ATMOS}$ and $\alpha_{P,SURF}$ via the isotropic SW model and calculate the implied ice albedo feedback from the relationship between α and $\alpha_{P,SURF}$. We will then compare this calculation with the ice albedo feedback calculated from the co-variability of TOA radiation and surface albedo (in the models) to see if the atmospheric absorption and reflection co-vary with the Arctic sea ice in the models (as our preliminary findings in the observations suggests). We will further analyze if the relationship between sea ice retreat and TOA radiation at the interannual timescale is the same as the models' response to external forcing. That is, are the cloud changes associated with the sea ice retreat at the interannual timescale:

A. A consequence of the ice retreat? In this case, the same cloud changes are expected to apply to the long term response to external forcing. Or,

B. Part of and/or emblematic of the processes that force the interannual variability of sea ice? In this case, the cloud changes are associated with the processes that force the ice retreat and have a non-casual statistical relationship with the ice extent that should not be expected to apply to the long term response to anthropogenic forcing.

By comparing the relationship between sea ice retreat and TOA radiation in the simulated (unforced) interannual variability with that in the response to external forcing, we can assess how much of the TOA radiative anomalies are a consequence of the ice retreat versus that which is due to other processes (i.e the mechanisms that force the ice retreat) to yield a better understanding of the ice albedo feedback. Specifically, we will compare the relationship between Arctic sea ice retreat and TOA radiation – measured as the change in Arctic averaged α_P per unit change in α – in a "typical" unforced ice retreat event within the PI simulation (the regression between α and α_P anomalies) with that in the change in long term means between the $4XCO_2$ simulation and PI simulation (the forced response). The end goal is to remove the component of the TOA radiation that is associated with the processes that force the natural variability of sea ice from our assessment of the ice albedo feedback since these processes will not contribute to the long term response to external (i.e. anthropogenic) forcing. Ultimately, the goal of this analysis is to develop a technique for calculating the impact of sea ice loss on TOA radiation – the ice albedo feedback– from interannual variability alone. The reason being, the observational record features large interannual variability and a small trend and the end goal of this work is refine our observational calculation of the ice albedo feedback using the statistics and physical based models.

Similarly, we will analyze if the models adequately represent the magnitude of year-to-year variability in F_{WALL} and its phase relationship to sea ice loss events. We can then ask if the same physical relationship between sea ice loss and F_{WALL} seen in the interannual (PI simulations) variability also applies to the long term relationship between Arctic ice loss and atmospheric circulation

($4XCO_2$). The hope of this analysis is that observational constraints on the relationship between sea ice loss, atmospheric circulation and Arctic radiation can be used as a metric to select a subset of GCMs that adequately simulate the Arctic climate system and, thus, will provide the most useful predictions of future Arctic climate change under global warming.

5 Relevance to NASA Goals

The proposed work will *utilize space-based remote sensing data* primarily from CERES, MODIS and CloudSAT/CALIPSO to investigate the connection between Arctic sea ice loss and the top of the atmosphere radiation budget. By doing so we will help *determine the mechanisms controlling the sea ice cover, including the quantification of the connection between sea ice and the atmosphere*. By quantifying the roles of clouds and atmospheric transport in the atmosphere from remote sensing observations and comparing the results to GCMs, the proposed research will *help improve predictive models* and *elucidate connections to the global system*. The research directly addresses the US Arctic Research Plan (2013-2017) program priorities of *"developing an integrated understanding of Arctic Atmosphere processes, their impact on the surface energy budget"* to which NASA is tasked to contribute.

6 Working timeline

Year one–analysis of co-variability of sea ice and clouds and methodological uncertainties

1. Analysis of MODIS and CALIPSO cloud fields that co-vary with sea ice retreat and validity of extending results to longer time period with APP-x data
2. Assess spatial extent of surface albedo anomalies in CERES versus other data sets
3. Assess performance of isotropic SW model in Arctic climate system against radiative transfer calculations

Year two –Variability of F_{WALL} and relationship with TOA radiation and sea ice retreat

1. Perform atmospheric energy transport calculations with MERRA2,NCEP and ERA reanalysis and check for consistency of the interannual variability between the different reanalyses
2. Analyze co-variability of F_{WALL} with sea ice, TOA radiation and the vertical profile of atmospheric temperature and humidity. Further analyze lead/lag relationships and the impact the vertical structure of F_{WALL} has on the atmosphere and its link to surface climate, cloud fields and TOA radiation.

Year three – General circulation model studies

1. Apply isotropic SW model to CMIP5 pre-industrial and $4XCO_2$ simulations. Analyze the Arctic surface albedo feedback from $\alpha_{P,SURF}$ and compare to that from the co-variability of α and α_P: do clouds co-vary with ice retreat as was suggested by the observations? Does interannual variability of ice albedo feedback and relationshiip between F_{WALL} and ice loss inform long term forced behavior?
2. Look for root cause of natural sea ice variability. Assess the roles of atmospheric and ocean energy transport into the Arctic and radiative processes by use of lead lag analysis. Does the atmospheric circulation remotely force sea ice loss or does it respond to sea ice anomalies?

References

Alexeev, V., P. Langen, and J. Bates (2005), Polar amplification of surface warming on an aquaplanet in ghost forcing experiments without sea ice feedbacks, *Climate Dyn.*, *24*(7), 655–666.

Baldwin, M., and T. Dunkerton (1998), Stratospheric harbingers of anomalous weather regimes, *Science*, *294*(5542), 581–584.

Bekrayev, R., I. Polyakov, and V. Alexeev (2010), Role of polar amplification in long-term surface air temperature variations and modern arctic warming, *J. Climate*, *23*, 3888–4006.

Blanchard-Wrigglesworth, E., K. Armour, C. Bitz, and E. DeWeaver (2011), Persistence and inherent predictability of arctic sea ice in a gcm ensemble and observations., *J. Climate*, *24*, 231–250.

Bony, S., et al. (2006), How well do we understand climate change feedback processes?, *J. Climate*, *19*, 3345–3482.

Burt, M., D. Rabdall, and M. Branson (2016), Dark warming, *J. Climate*, *29*, 705–719.

Cao, Y., S. Liang, X. Chen, and T. He (2015), Assessment of sea ice albedo radiative forcing and feedback over the northern hemisphere from 1982 to 2009 using satellite and reanalysis data, *J. Climate*, *27*, doi:doi.org/10.1175/JCLI-D-14-00389.1.

Choi, Y.-S., B.-M. Kim, S.-K. Hur, S.-J. Kim, J.-H. Kim, and C.-H. Ho (2014), Connecting early summer cloud-controlled sunlight and late summer sea ice in the arctic, *J. Geophys. Res.*, *119*, doi:10.1002/2014JD022013.

Dee, D., et al. (2011), The era-interim reanalysis: configuration and performance of the data assimilation system, *Quart. J. Roy. Meteor. Soc.*, *137*, 553–597.

Deser, C., R. Tomas, and L. Sun (2015), The role of oceanŰatmosphere coupling in the zonal-mean atmospheric response to arctic sea ice loss, *J. Climate*, *28*, 2168–2186.

Ding, Q., J. Wallace, D. Battisti, E. Steig, A. Gallant, H. Ki, and L. Geng (2014), Tropical forcing of the recent rapid arctic warming in northeastern canada and greenland, *Nature*, *509*, 209–214.

Ding, Q., et al. (2017), Influence of high-latitude atmospheric circulation changes on summertime arctic sea ice, *Nat. Clim. Chang.*, *7*, 289–295.

Donohoe, A., and D. Battisti (2011), Atmospheric and surface contributions to planetary albedo., *J. Climate*, *24*(16), 4401–4417.

Donohoe, A., and D. Battisti (2013), The seasonal cycle of atmospheric heating and temperature, *J. Climate*, *26*(14), 4962–4980.

Francis, J., and S. Vavrus (2012), Evidence linkin arctic amplification to extreme weather in midlatitudes, *Geophys. Res. Lett.*, *39*(L06801), 10.1029/2012GL051,000.

Fu, Q., and K. Liou (1993), Parameterization of the radiative properties of cirrus clouds, *J. Atmos. Sci.*, *50*, 2008–2025.

Gelaro, R., et al. (2017), The modern-era retrospective analysis for research and applications, version 2 (merra-2), *J. Climate*.

Holland, M. M., and C. Bitz (2003), Polar amplification of climate in coupled models., *Climate Dyn.*, *21*, 221–232.

Hwang, Y., D. Frierson, and J. Kay (2011), Coupling between arctic feedbacks and changes in poleward energy transport, *Geophys. Res. Lett.*, *38*, L17,704.

Kalnay, E., et al. (1996), The NCEP/NCAR 40-year reanalysis project., *Bull. Amer. Meteor. Soc.*

Kato, S., N. Loeb, P. Minnis, J. Francis, T. Charlock, D. Rutan, E. Clothiaux, and S. Sun-Mack (2006), Seasonal and interannual variations of top-of-atmosphere irradiance and cloud cover over polar regions derived from ceres data set., *Geophys. Res. Lett.*, *33*, doi:10.1029/2006GL026,685.

Kato, S., et al. (2011), Improvements of top-of-atmosphere and surface irradiance computations with calipso-, cloudsat-, and modis-derived cloud and aerosol properties, *J. Geophys. Res.*, *116*(D19), doi:doi:10.1029/2006GL026685.

Kay, J., M. Holland, C. Bitz, E. Blanchard-Wrigglesworth, A. Gettelman, A. Conley, and D. Bailey (2012), The influence of local feedbacks and northward heat transport on the equilibrium arctic climate response to increased greenhouse gas forcing, *J. Climate*, *25*, 5433–5450.

Kay, J. E., T. L'Ecuyer, A. Gettelman, G. Stephens, and C. O'Dell (2008), The contribution of cloud and radiation anomalies to the 2007 arctic sea ice extent minimum, *Geophys. Res. Lett.*, *35*(L08503), doi:10.1029/2008GL033451.

Key, J. (2002), *The cloud and surface parameter retrieval (CASPR) system for polar AVHRR*, Cooperative Institute for Meteorological Satellite Studies, University of Wisconsin, Madison.

Key, J., and A. Schweiger (1998), Tools for atmospheric radiative transfer: Streamer and fluxnet, *Comput. Geosci.*, *24*, 443–451.

Kratz, D. P., S. K. Gupta, A. C. Wilber, and V. E. Sothcott (2010), Validation of the ceres edition 2b surface-only flux algorithms., *J. Appl. Meteor.*, *49*, 164–180.

Liu, Y., S. Ackerman, B. Maddux, J. Key, and R. Frey (2010), Errors in cloud detection over the arctic using a satellite imager and implications for observing feedback mechanisms, *J. Climate*, *23*(7), 1894–1907.

Lorenz, E. (1953), A multiple index notation for describing atmospheric transport processes.

Lucht, W. (1998), Expected retrieval accuracies of bidirectional reflectance and albedo from eos-modis and misr angular sampling, *J. Geophys. Res.*, *103*, 8763–8778.

Overland, J., and P. Turet (1994), Variability of the atmospheric energy flux across 70°n computed from the gfdl data set., *Centennial Volume, Geophys. Monogr.*, *84*, 313–325.

Overland, J., J. Francis, R. Hall, E. Hanna, S.-J. Kim, and T. Vihma (2015), The melting arctic and midlatitude weather patterns: Are they connected?, *J. Climate*, *28*, 7917–7932.

Pistone, K., I. Eisenman, and V. Ramanathan (2014), Observational determination of albedo decrease caused by vanishing arctic sea ice, *Proc. Nat. Acad. Sci. USA*, *111*(9), 3322–3326.

Platnick, S., M. King, S. Ackerman, W. Menzel, B. Baum, J. Riedi, and R. Frey (2003), The modis cloud products: Algorithms and examples from terra, *IEEE Trans. Geosci. Remote Sens.*, *41*(2), 459–473.

Qu, X., and A. Hall (2005), Surface contribution to planetary albedo variability in the cryosphere regions., *J. Climate*, *18*, 5239–5252.

Rosel, A., L. Kaleschke, and G. Birnbaum (2012), Melt ponds on arctic sea ice determined from modis satellite data using an artificial neuronal network, *6*, 431–446.

Rutan, D., F. Rose, N. Smith, and T. Charlock (2001), Validation data set for CERES surface and atmospheric radiation budget (SARB), *WCRP/GEWEX Newsletter*, *11*(1), 11–12.

Rutan, D., T. Charlock, F. Rose, S. Kato, S. Zentz, and L. Coleman (2006), Global surface albedo from ceres/terra surface and atmospheric radiation budget(SARB) data product, *In Proceedings of 12th Conference on Atmospheric Radiation (AMS)*, *11*(1), 11–12.

Schaaf, C., et al. (2002), First operational brdf, albedo nadir reflectance products from modis, *Remote Sensing of Environment*, *83*.

Schweiger, A., R. Lindsay, S. Vavrus, and J. Francis (2008), Relationships between arctic sea ice and clouds during autumn, *J. Climate*, *21*(18), 4799–4810.

Serreze, M., A. Barrett, A. Slater, M. Steele, J. Zhang, and K. Trenberth (2007), The large-scale energy budget of the arctic, *J. Geophys. Res.*, *112*, doi:10.1029/2006JD008230.

Soden, B., and I. Held (2006), An assessment of climate feedbacks in coupled oceanŰatmosphere models, *J. Climate*, *19*, 3354–3360.

Steele, M., J. Zhang, and W. Ermold (2010), Mechanisms of summertime upper arctic ocean warming and the effect on sea ice melt, *J. Geophys. Res.*, *115*, doi:10.1029/2009JC005849.

Stephens, e. a., G. L. (2008), Cloudsat mission: Performance and early science after the first year of operation, *J. Geophys. Res.*, *113*(D00A18), doi:10.1029/2008JD009982.

Taylor, K., R. Stouffer, and G. Meehl (2012), An overview of cmip5 and the experiment design., *Bull. Amer. Meteor. Soc.*, *93*, 485–498.

Trenberth, K. E., and D. P. Stepaniak (2003), Co-variability of components of poleward atmospheric energy transports on seasonal and interannual timescales., *J. Climate*, *16*, 3691–3705.

Uttal, T., et al. (2002), Surface heat budget of the arctic ocean, *Bull. Amer. Meteor. Soc.*, (83), 255–275.

Varvus, S., F. Wang, J. Francis, Y. Peings, and J. C. and (2017), Changes in north american atmospheric circulation and extreme weather: Influence of arctic amplification and northern hemisphere snow cover, *J. Climate*, *29*, doi:doi.org/10.1175/JCLI-D-16-0762.1.

Wang, X., and J. Key (2005), Arctic surface, cloud, and radiation properties based on the avhrr polar pathfinder dataset. part i: Spatial and temporal characteristics, *J. Climate*, *18*, 2558–2574.

Woods, C., and R. Caballero (2016), The role of moist intrusions in winter arctic warming and sea ice decline, *J. Climate*, *29*(12), 4473–4485.

Zhang, J., R. Lindsay, A. Schweiger, and M. Steele (2013), The impact of an intense summer cyclone on 2012 arctic sea ice retreat, *Geophys. Res. Lett.*, *40*(4), 720–726.